Publ. Astron. Soc. Japan **38**, 347–360 (1986)

Giant Stellar-Wind Shell Associated with the H II Region M16*

Yoshiaki SOFUE and Toshihiro HANDA

Nobeyama Radio Observatory, Minamimaki-mura, Minamisaku-gun, Nagano 384–13*
and
Department of Astronomy, Faculty of Science, University of Tokyo, Bunkyo-ku, Tokyo 113

and

Ernst FÜRST, Wolfgang REICH, and Patricia REICH

Max-Planck-Institut für Radioastronomie, Auf dem Hügel 69, D-5300 Bonn 1, FR Germany

(Received 1985 August 14; accepted 1985 December 12)

Abstract

Radio continuum observations at 2.7 and 10 GHz of the star forming complex M16 revealed a large loop of diameter 1°.2 (60 pc) with a flat (thermal) spectrum. The loop is likely to be a shell of H II gas which expands from M16 toward the south. Optical (Hα) filaments are found associated with this loop. An H I shell of diameter 70 pc is found surrounding continuum shell, and is expanding at a velocity of 4 km s^{-1}. A giant molecular cloud is located in contact with the northern edge of the shell. A stellar-wind-bubble model is proposed for the formation of the shell, in which the rate of kinetic energy injection from the central O stars is estimated to be 3.3×10^{36} erg s^{-1} and the corresponding mass-loss rate $2.6\times10^{-6}M_{\odot}$ yr^{-1} with an age of the shell of about 7×10^{6} yr. Blocking by the giant molecular cloud may have caused the one-sided expansion of the bubble. A relationship of M16 and its bubble to the star forming complex M17 is suggested.

Key words: H II regions; Interstellar matter; Radio emission; Star formation; Stellar wind.

1. Introduction

Active star forming complexes are often associated with giant shells. A typical example is seen in the Orion complex, which has the Barnard loop and an H I shell called the Eridanus loop (Reynolds and Ogden 1979). Many similar H II rings are shown to exist in the Large Magellanic Clouds (Elliot et al. 1978). Such a loop

* Based on observations made at the Nobeyama Radio Observatory (NRO). NRO, a branch of the Tokyo Astronomical Observatory, University of Tokyo, is a facility open for general use by researchers in the field of astronomy and astrophysics.

structure, or a superbubble, may be formed by an intense energy injection from the central OB stars into the interstellar gas through a high rate of mass loss or supernova explosions (Weaver et al. 1977; Conti 1978; McCray and Snow 1979; Tomisaka et al. 1981). The shells are defined as a loop on the sky of enhanced H I, Hα, and/or X-ray emissions. However, except for the radio continuum study of the Barnard loop by Reich (1978), few radio continuum detections of such superbubbles are made as yet because of the difficulty due to very low surface brightness and confusion with the galactic background radiation (Sofue and Nakai 1983). In fact the Barnard loop has a diameter of 115 pc and extends over 14° on the sky (Reich 1978).

Study of further examples of such shell structures around star forming regions in the radio continuum and H I and/or CO line emissions will give a useful clue to investigate the behavior of gases surrounding OB stars and H II regions. We may be able to learn about how the released energy by young massive stars is reduced to the interstellar gas. In the present paper we report the detection of a giant radio continuum shell associated with the bright H II region M16, which is one of the most active star forming sites in the Sagittarius arm.

2. Radio Continuum Shell

We have noticed a large loop associated with M16 through an inspection of the radio continuum survey data of the galactic plane at 2.7 GHz recently published by Reich et al. (1984) (figure 1), and of that of a 10-GHz survey being carried out at NRO. The observations at 2.7 GHz were made using the 100-m telescope of MPIfR in Bonn, and the HPBW was 4′.3. The 10-GHz observations were made in 1984 using the 45-m telescope of NRO as part of the galactic plane survey, and the HPBW was 2′.7. Details of the observations are given by Reich et al. (1984) and Sofue et al. (1984).

Figure 2a shows a region of 1°.5×1°.5 centered on G16.4+0.7 in the radio continuum emission at 2.7 GHz. In this figure large-scale structures with scale sizes greater than 0°.3 have been subtracted from the original map using the BGF (background filtering) technique of Sofue and Reich (1979). Therefore, fine ridges and small-size sources are more clearly enhanced in this figure compared with the original map which is dominated by the strong galactic background radiation with steep gradient. Figure 2b shows the same but in a gray-scale representation. Figure 3 shows a 10-GHz map of the same region after smoothing to a HPBW of 4′.3, where the background emission has been again subtracted using the BGF method.

In the figures, in particular at 2.7 GHz, we can see a large loop of radio enhancement. The loop is elongated in the direction parallel to the galactic plane. The center position is at (l, b)=(16°.4, 0°.7) (=G16.4+0.7) and the major and minor diameters are 1°.2 and 0°.9, respectively. Inside the loop we can see two other smaller loops: one is centered on G16.6+0.8 and the diameter is 0°.8 again slightly elongated in the direction parallel to the galactic plane. The other is found centered on G16.7+0.8 and the diameter is about 0°.5 with its brightest part at G16.5+1.0 which connects itself to the bright arc running from M16 toward SW.

On the red print of the Palomar Sky Survey (figure 4) we find thin filamentary nebulosities composing a large loop structure coinciding in position and appearance

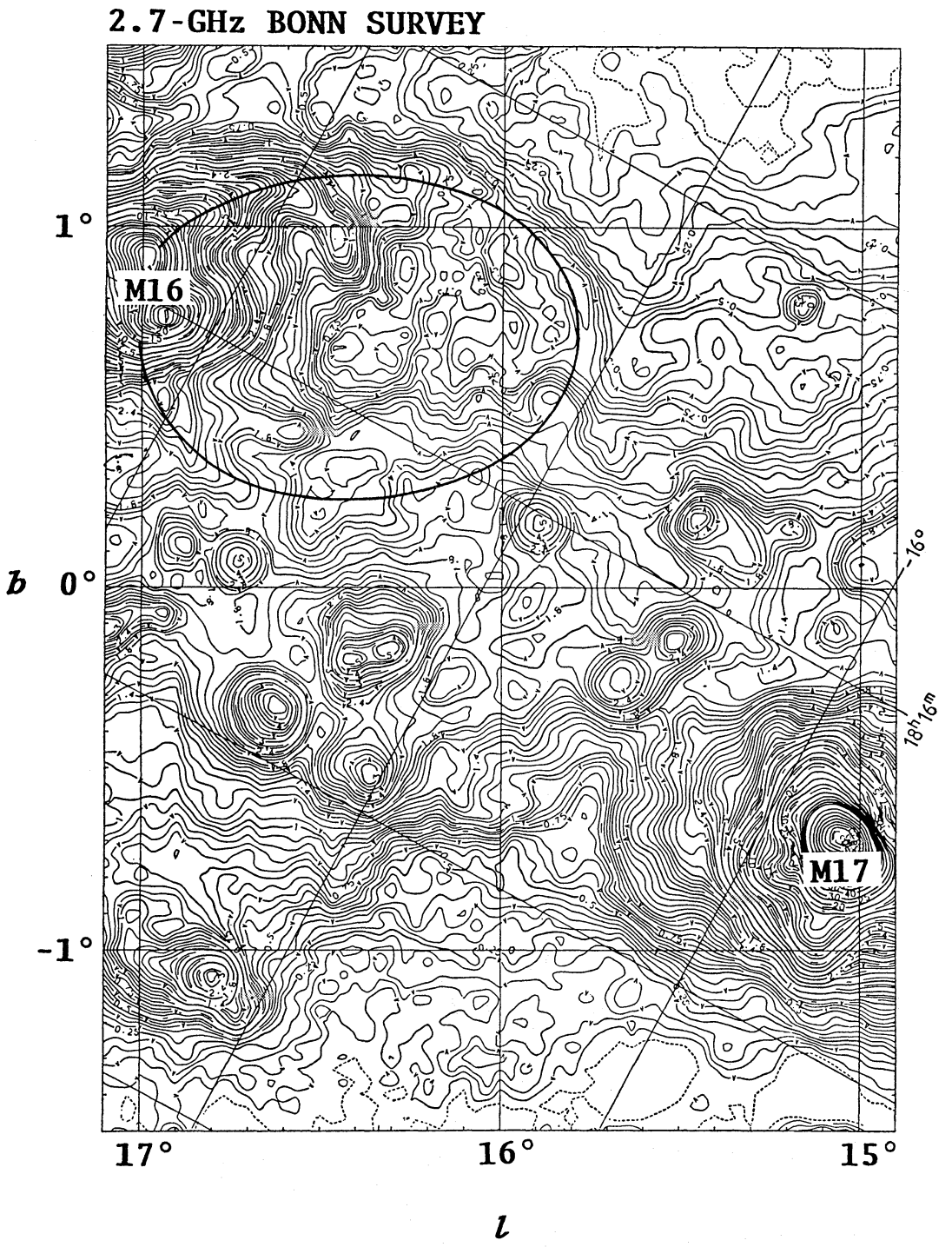

Fig. 1. Reproduction of the G15–G17 region from the 2.7-GHz Bonn survey (Reich et al. 1984). The contour numbers are in units of K T_b. Note a loop feature associated with the H II region M16 as indicated with the line.

with the present radio loop. The inner smaller loops are also clearly recognized on the photograph. The optical emission line maps of this region by Parker et al. (1979) indicate that the filaments are mostly due to Hα emission. The photographic and radio appearances of the loop indicate its physical connection to the M16 complex.

The LSR velocities at several peaks in M16 have been measured by H110α re-

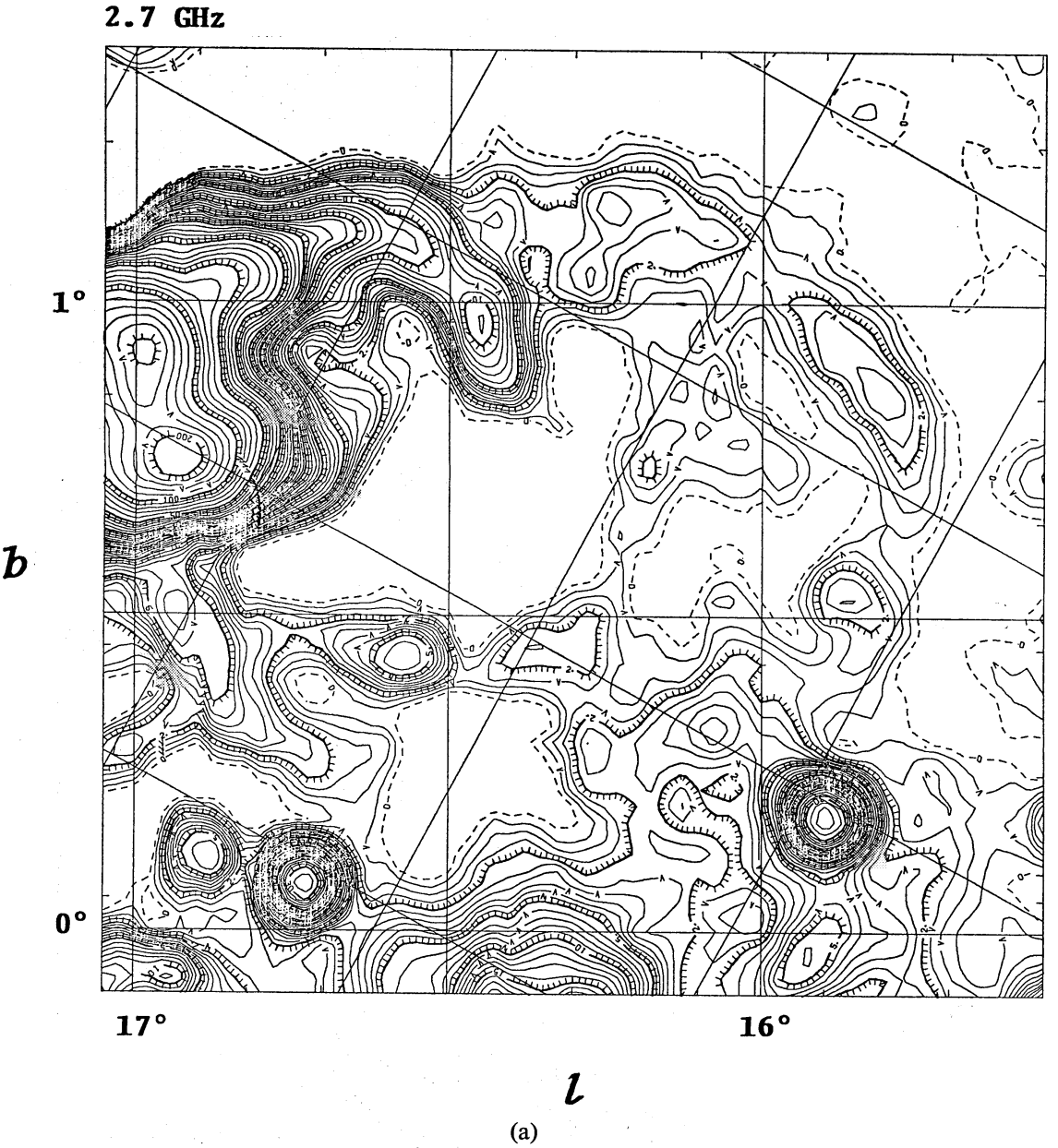

(a)

Fig. 2a. Brightness distribution of the M16 shell at 2.7 GHz obtained from the Bonn survey data (Reich et al. 1984) after background filtering. The contour numbers are in units of 2.23×10^{-22} W m^{-2} sr^{-2} Hz^{-1} or 100 mK T_b.

combination line observations by Downes et al. (1980). They give V_{LSR}=28.0, 23.5, and 25.5 km s^{-1}, respectively, at G16.95+0.80, G16.98+0.83, and G16.98+0.92. The kinematical distance to M16 is then about 2.8 kpc. If the radio loop is associated with M16, the major diameter is about 59 pc. This diameter is half that of the Barnard loop, and is one fourth of the Eridanus loop. The loop ridge is not well resolved in the present observations, and this leads to an upper limit of the shell thickness of 3.5 pc, or the line-of-sight depth tangentially through the shell is less than 30 pc.

It is difficult to determine the total flux density of the region contained by the loop because of the contamination by the strong background radiation. The situation

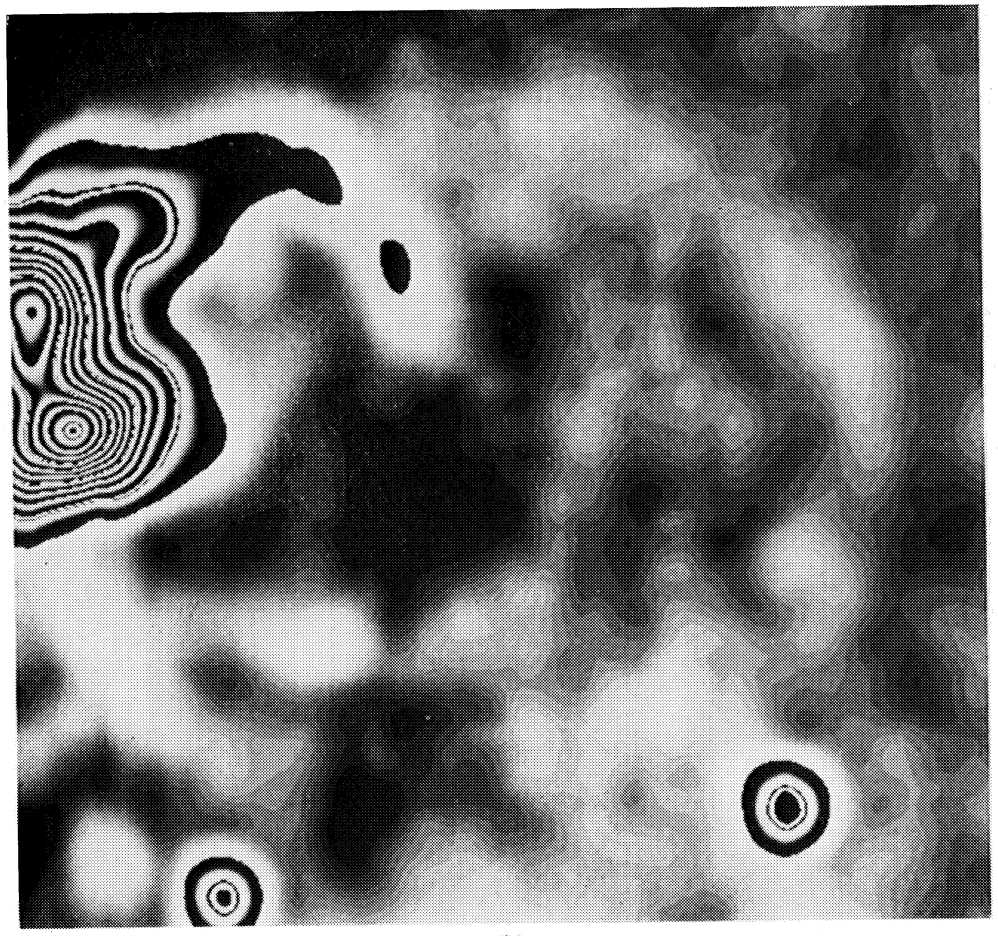

(b)

Fig. 2b. The same as figure 2a but in a gray-scale representation.

can be well understood by looking at the original survey map at 2.7 GHz (figure 1). However, we can determine fairly well the contribution from the loop ridge alone using the BGF map, which is not disturbed significantly by the background. In the following we discuss the features appearing on the BGF maps.

The radio spectrum of the surface brightness on the loop ridge as determined from the 2.7- and 10-GHz BGF maps is flat, which indicates a thermal gas origin of the loop likely to be a shell composed of H II gas. This is consistent with its associated Hα emission. The excess brightness temperature of the shell ridge at 2.7 GHz is about 0.2 K at the position G15.8+0.8, where the outer shell is most clearly seen. The emission measure (EM) can be calculated using the formula given by Mezger and Henderson (1967). By assuming an electron temperature of 10^4 K for a typical diffuse H II gas, we obtain $EM \cong 500$ pc cm^{-6}. Since the line-of-sight depth is about 30 pc or less, the electron density is about $n_e = 4.1$ cm^{-3} or larger. Since the brightness along the outer shell is almost constant over a large range of the loop, we may very roughly estimate the total mass of the ionized hydrogen involved in the shell; we take here the diameter along the major and minor axes as 59 pc (1°.2) and 44 pc (0°.9), respectively, and the thickness of 3 pc. Assuming a uniform density of the order of $n_e = 4$ cm^{-3} over the shell, we obtain a total H II mass as $M_{\mathrm{H\,II}} = 4\pi R^2 dR n_e m_{\mathrm{H}}$

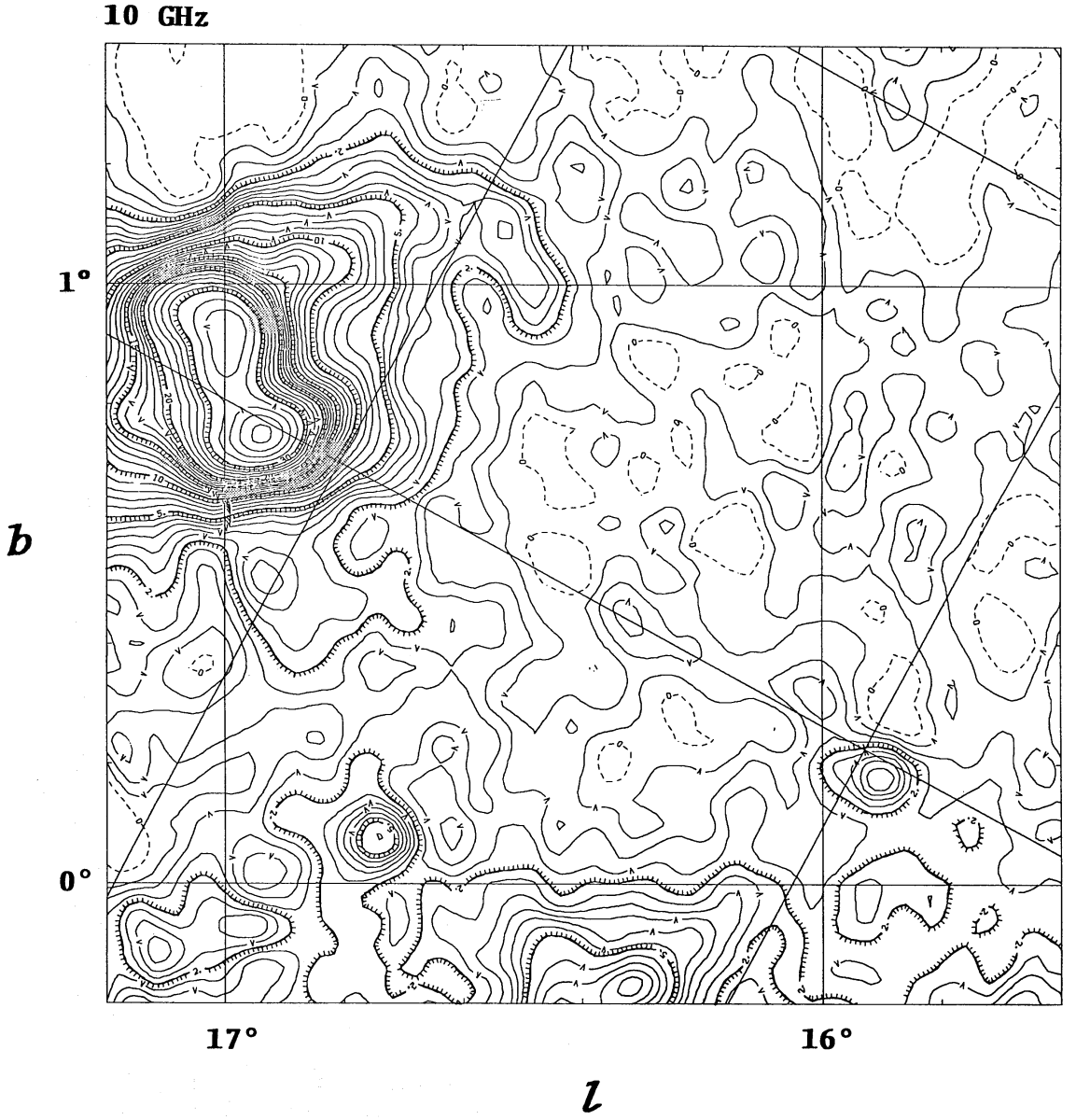

Fig. 3. The same as figure 2 but at 10 GHz taken with the 45-m telescope and smoothed to a HPBW of 4′.3. The contour numbers are in units of 10^{-21} W m^{-2} sr^{-1} Hz^{-1} or 30 mK T_b.

with $R=(59\text{ pc}\times 44\text{ pc})^{1/2}/2=25$ pc and $dR=3$ pc. Then we obtain $M_{\text{H II}}=2.5\times 10^3 M_\odot$. The thermal energy involved in the shell is approximately $E_{\text{th}}=(3/2)\,R_g M_{\text{H II}} T=6\times 10^{48}$ erg with $T=10^4$ K, where R_g is the gas constant.

3. H I and CO Gases

In order to see if the present radio continuum loop is associated with atomic and molecular hydrogen gases and to get information about its motion, we examine published H I and CO survey data of the galactic plane region.

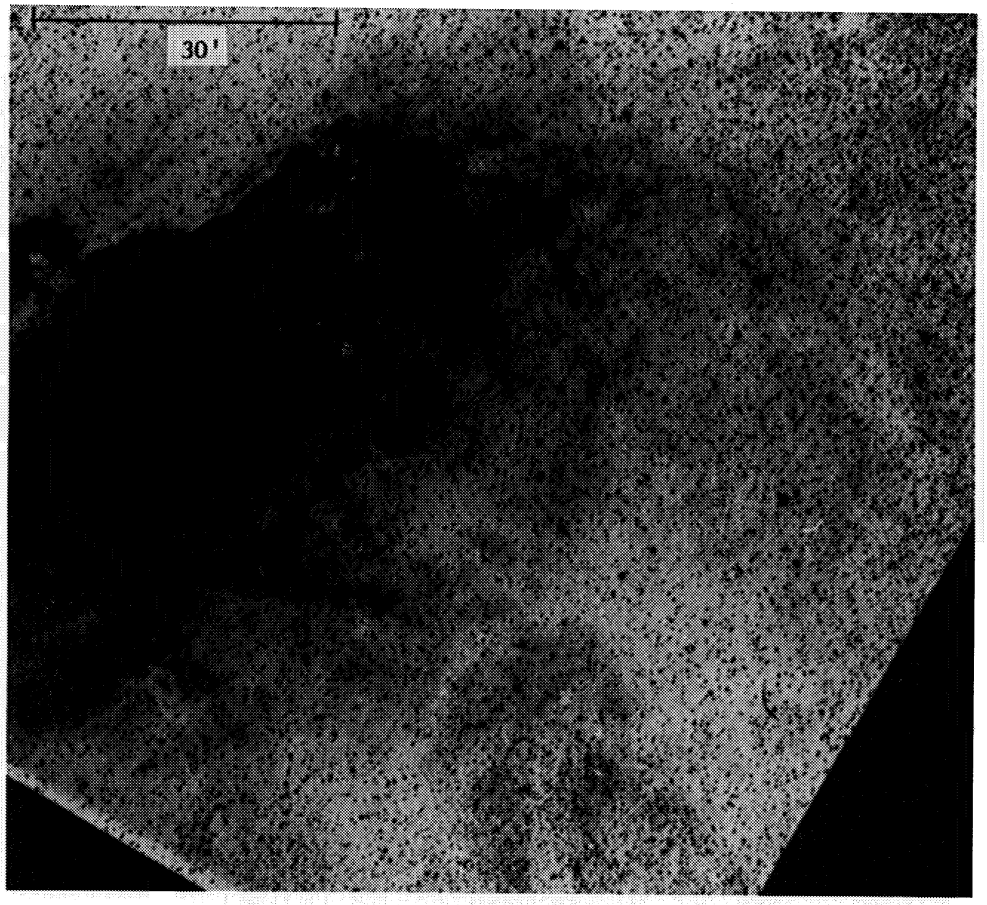

Fig. 4. Reproduction of the Palomar red print for about the same region as figure 3, showing the optical filaments composing a loop structure associated with M16, which coincides in position and appearance with the radio loop. (© 1960 National Geographic Society–Palomar Sky Survey. Reproduced by permission of the California Institute of Technology.)

(i) H I Shell

We make use of the Maryland-Greenbank H I line survey (Westerhout et al. 1982). To see if the loop is associated with the H I gas at a distance of 2.8 kpc, or at V_{LSR}=20–30 km s^{-1}, we make brightness temperature maps at V_{LSR}=20, 25, and 30 km s^{-1}. The maps are shown in figure 5 in the form of contour diagrams. The strong continuum emission of M16 causes a strong absorption feature near G17+0.8, especially at V_{LSR} 30 km s^{-1}, which makes it difficult to see the H I structure near M16. However, at positions far enough from M16 we can see a looplike structure surrounding a depression of the H I emission at around G16.3+0.6. The H I loop is most clearly seen at V_{LSR}=25 and 30 km s^{-1}. Although the lower angular resolution of the H I observations (13′) gives only a rough idea about the association, the western ridge seems to coincide with the western ridge of the continuum shell. The southern and southwestern parts of the H I loop lie slightly outside the continuum loop. The major and minor diameters of the H I loop are 1°.4 (68 pc) and 1°.1 (54 pc), respectively. The shell ridge is not resolved with the present beam width and this leads to a shell thickness less than 10 pc.

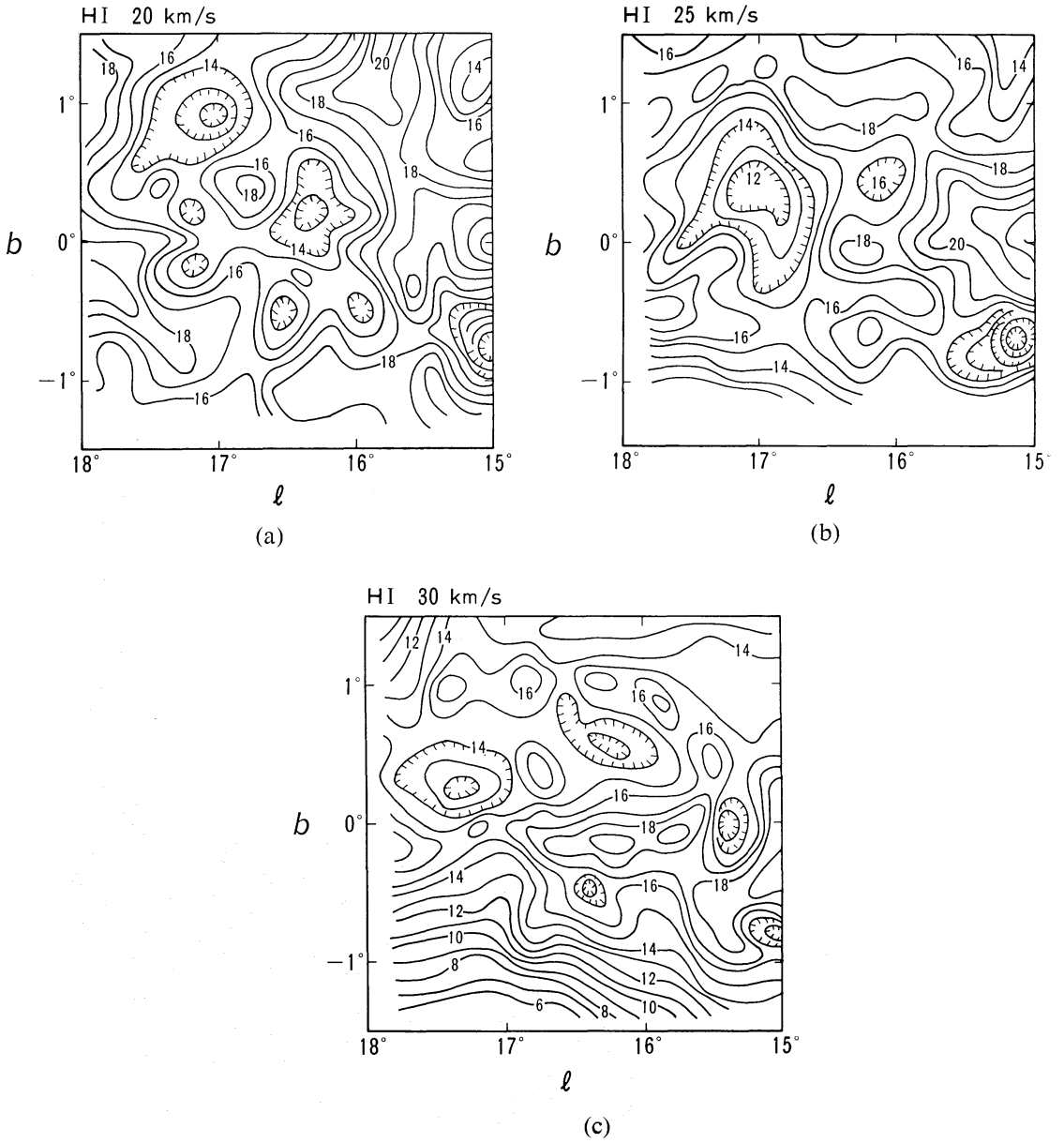

Fig. 5. Distributions of H I brightness temperature around the M16 shell at $V_{LSR}=20$, 25, and 30 km s^{-1}. The contour numbers are in units of 5 K T_b.

We show in figure 6 velocity–latitude diagrams of H I brightness temperature, $T_b(b, v)$, for the region containing our object, $15^\circ.8 \leq l \leq 16^\circ.6$ and $1^\circ.3 \geq b \geq 0^\circ$. We used again the data of Westerhout and Wendlandt (1982). We find a remarkable shell on the b–v plane at $l=16^\circ.0$ to $16^\circ.4$, particularly at $l=16^\circ.2$. The shell is composed of two sharp ridges at $V_{LSR}=24$ and 32 km s^{-1} with a deep hole centered on $V_{LSR}=28$ km s^{-1} and $b=0^\circ.6$. Figure 7 shows the cross sections of the shell at $b=0^\circ.6$ for $l=15^\circ.8$, $16^\circ.2$, and $16^\circ.6$. From these figures we can see that the shell is expanding at $V_{exp}=4$ km s^{-1} (half the velocity difference between the higher and lower velocities) along the line of sight on $(l, b)=(16^\circ.2, 0^\circ.6)$, and the velocity dispersion in the shell is about $\sigma=4$ km s^{-1}. Assuming a constant expansion velocity, the age of the shell is

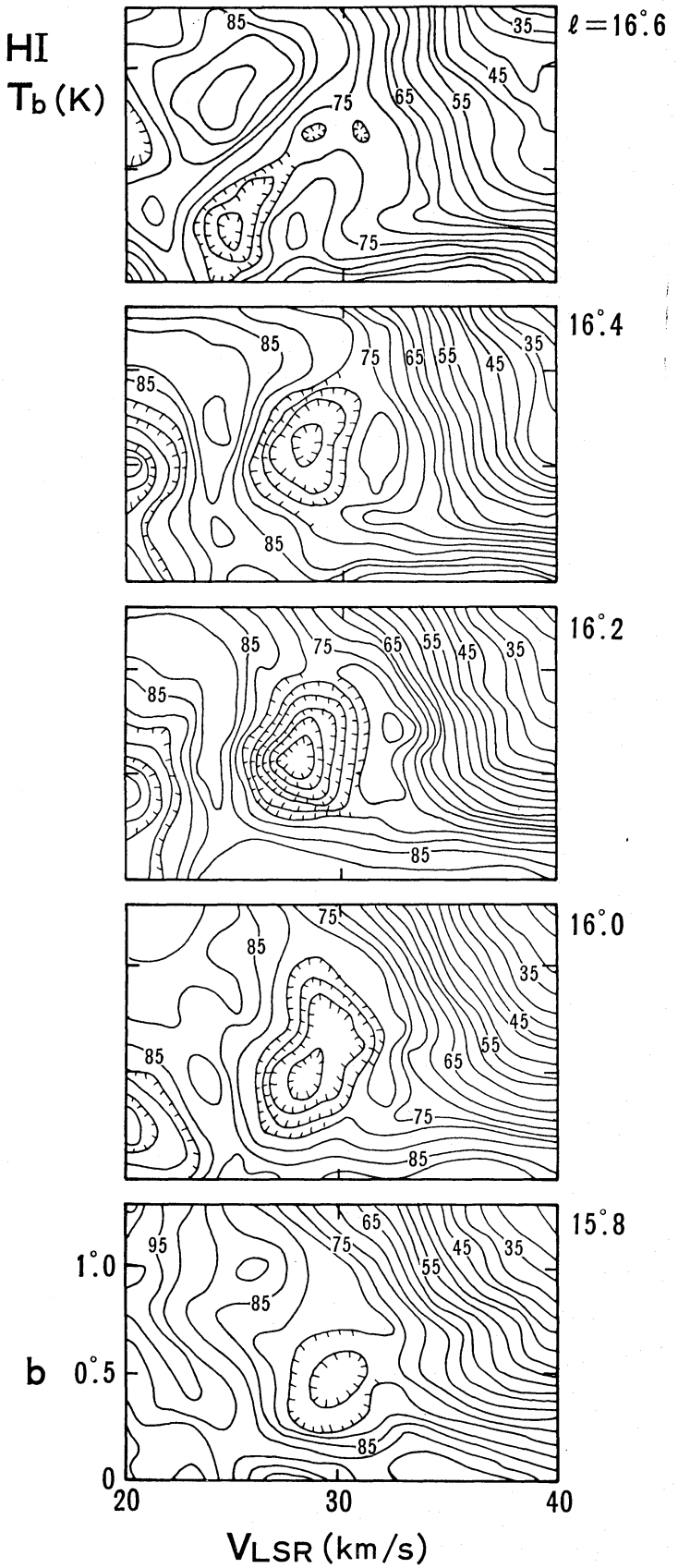

Fig. 6. H I $T_b(b, v)$ diagrams at $l=15°.8$ through $16°.6$ obtained from Westerhout and Wendlandt (1982). The contour numbers are in units of 1 K T_b.

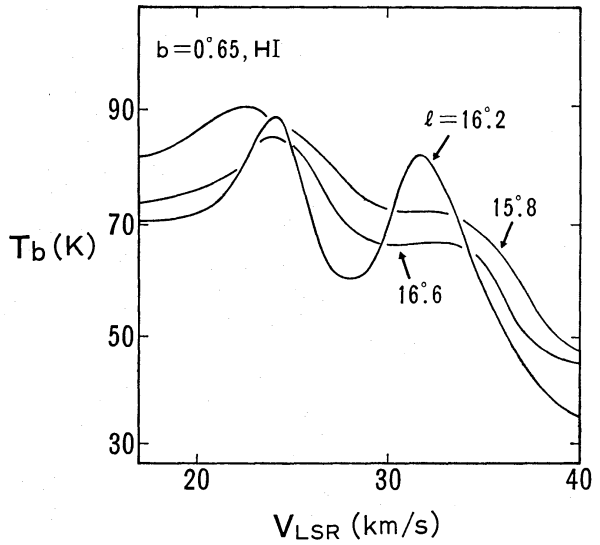

Fig. 7. H I line profiles along $b=0^{\circ}.65$ at $l=15^{\circ}.8$, $16^{\circ}.2$, and $16^{\circ}.6$.

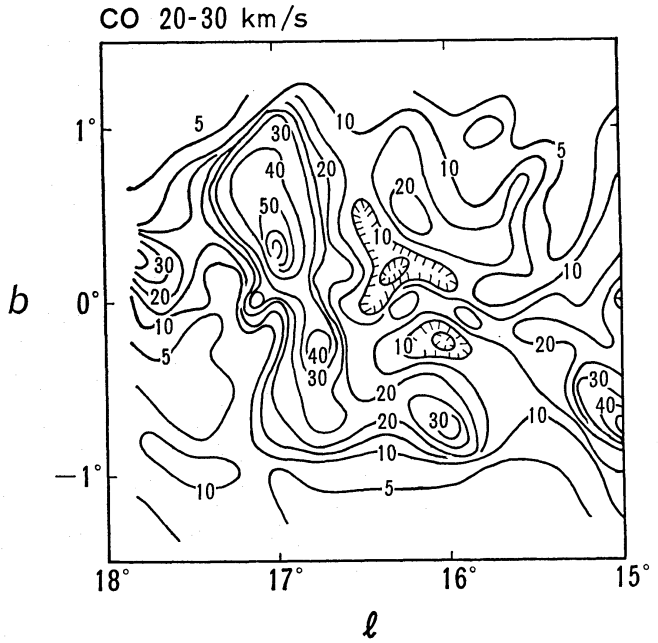

Fig. 8. Integrated intensity map of the ^{12}CO ($J=1$–0) line emission made from the Columbia survey (Dame 1984). The contour numbers are in units of K km s^{-1}.

estimated to be $t=7\times10^{6}$ yr. The column density of the shell toward this position is calculated (e.g., Kerr 1968) to be about $N_{\rm H\,I}\approx1.5\times10^{20}$ cm^{-2} by taking the excess of the peak brightness temperature as 20 K and the velocity width of 4 km s^{-1}. If the shell has a uniform radial column density of this amount, the total H I mass is estimated as about $M_{\rm H\,I}=10^{4}M_{\odot}$, and the H I number density in the shell is larger than 5 cm^{-3}. The kinetic energy of the shell due to the expanding motion is then about $E_{\rm k}=(1/2)M_{\rm tot}V_{\rm exp}^{2}=2\times10^{48}$ erg, where $M_{\rm tot}=M_{\rm H\,II}+M_{\rm H\,I}$. The kinetic energy is comparable to the thermal energy of the H II gas in the shell. The present energy amount

Table 1. Radio shell associated with M16.

Center position	$l=16\overset{\circ}{.}4$, $b=0\overset{\circ}{.}7$
	R. A. (1950)=$18^{h}15\overset{m}{.}3$, Decl. (1950)=$-14\overset{\circ}{.}4$
Distance	2.8 kpc
Major diameter (continuum/H I)	$1\overset{\circ}{.}2$ (59 pc)/$1\overset{\circ}{.}4$ (68 pc)
Minor diameter (continuum/H I)	$0\overset{\circ}{.}9$ (44 pc)/$1\overset{\circ}{.}1$ (54 pc)
Shell thickness (continuum/H I)	$\lesssim$3 pc/$\lesssim$10 pc
Radio spectrum	Flat (thermal)
V_{LSR} of H I shell center	28 km s^{-1}
Expansion velocity	4 km s^{-1}
Velocity dispersion in shell	4 km s^{-1}
Age (=radius/expansion velocity)	7×10^{6} yr
H II density	$\gtrsim$4 cm^{-3}
H I density	$\gtrsim$5 cm^{-3}
H II mass	$2.5\times10^{3}M_{\odot}$
H I mass	$\sim10^{4}M_{\odot}$
Total mass	$\sim10^{4}M_{\odot}$
Kinetic energy of shell	$\sim2\times10^{48}$ erg
Thermal energy of shell	$\sim6\times10^{48}$ erg

and expansion velocity are much smaller than those obtained for the Orion-Eridanus shell (Reynolds and Ogden 1979) and for H I supershells (Heiles 1979).

(ii) CO Gas Distribution

We make use of the Columbia ^{12}CO-line survey (Dame 1984) to construct CO intensity maps in order to compare with the H I and continuum maps. Figure 8 shows the distribution of CO intensity integrated between $V_{LSR}=20$ and 30 km s^{-1} in the form of a contour map. We find two dense clouds associated with M16 and M17 at G17+0.5 and G15−0.7, respectively. However, the association of the molecular gas with the radio shell is not clear from this figure. We note that the giant molecular cloud G17+0.5 is located in contact with the northeastern edge of the shell. This fact suggests that the expansion of the shell is blocked by this cloud in the NE side and the ejected material from M16 has been directed toward SW to produce a shell asymmetric with respect to the energy injection center.

4. Discussion

The structure of the shell observed here agrees with that predicted by the "stellar wind bubble" model (Weaver et al. 1977; McCray and Snow 1979; Tomisaka et al. 1981): the innermost region of the shell is a cavity dominated by a stellar wind from early-type stars and is bounded by a shocked H II gas. The H II shell thus formed is observed as the thermal radio emission loop. The outermost region is further surrounded by a cooled H I shell consisting of swept interstellar material. Tomisaka et al. (1981) have shown through their numerical simulation that the shell radius, R_{B}, of such a wind bubble is given by

$$R_{B}(\mathrm{pc})=17.5(L_{k}/10^{36}\ \mathrm{erg\ s^{-1}})^{0.22}(n\ \mathrm{cm^{-3}})^{-0.29}(t/10^{6}\ \mathrm{yr})^{0.49}\ ,$$

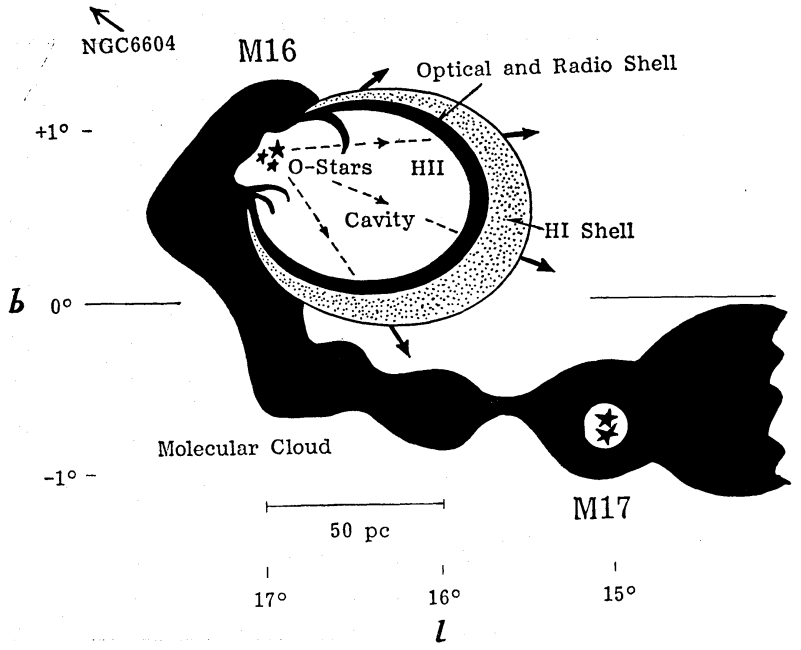

Fig. 9 Schematic illustration of the relationship of the optical, radio-continuum, and H I shells to the star forming sites M16 and M17 and to the associated molecular clouds.

where L_k is the ejection rate of kinetic energy from the central OB stars in a strong wind phase, or $L_k=(1/2)\dot{M}_w V_w^2$ with M_w the mass-loss rate and V_w the initial wind velocity, n is the number density of ambient material, and t is the age of the shell.

With the estimated age of 7×10^6 yr, the radius of $R_B=60$ pc, which is an approximate distance to the farthermost part of the shell from the M16 core, and an assumed ambient gas density of $n=1$ cm^{-3}, we obtain $L_k=3.3\times10^{36}$ erg s^{-1}. Taking a typical wind velocity as $V_w=2000$ km s^{-1} (Conti 1978; Tomisaka et al. 1981), we have $\dot{M}_w=2.6\times10^{-6}M_\odot$ yr^{-1}. This amount of mass loss is close to a typical mass-loss rate of an O star in an active wind phase (Conti 1978). Thus the formation of the M16 shell may be naturally attributed to a giant stellar wind bubble being driven by the mass loss from one or a few O stars in the core of the M16 complex. The total kinetic energy ejected from the stars is evaluated as $E_w=L_k t\sim7\times10^{50}$ erg. The total energy involved in the shell at present is about $E=E_k+E_{th}\sim10^{49}$ erg, and therefore only a small fraction of the ejected energy has been given to the heating and acceleration of the shell.

The M16 shell seems similar in size and appearance to the Barnard loop (Reynolds and Ogden 1979; Reich 1978). However, the difference between the two is that the Barnard loop surrounds the Orion complex in a rather circularly symmetric way, while the M16 shell is located on one side of the exciting stars and seems to expand towards the south only. The asymmetric expansion may be due to blocking by the giant molecular cloud lying at $(l, b)=(17°, 0°.5)$ on the NE edge of the shell as seen in figure 8.

In figure 9 we illustrate the schematic relationship of the optical, radio, and H I shells and the molecular clouds associated with the M16 complex. The figure shows also the position of the M17 star forming region and its associated molecular clouds,

which are located at about the same distance as M16 from the sun (2.5 kpc). Elmegreen (1980) suggests that a molecular cloud at $l=13°$, which contains a far-IR source (region III in his term), may be a future star forming site next to M17 and will make a string of "beads" of star forming sites with M16 and M17. We note that there exists another H II region, NGC 6604, to the north of M16 at about the same angular distance to M17. In fact the Hα photograph of Parker et al. (1979) of this region reveals a string of three H II regions, NGC 6604, M16, and M17, from north to south along a line inclined by about 20° with the galactic plane. These three H II regions are in the order from more extended to compact and therefore from an older (NGC 6604) to a new (M17) star forming site with M16 in between. If we include the possible "future" star forming site (region III), we may have a long string of beads of star forming activity in the Sagittarius arm from $l=13°$ through $l=19°$ over 6° on the sky or over a projected distance of 300 pc.

The alignment in the order of the age from older to younger suggests that there may have been a sequential star forming activity along this long string. The initial star formation took place in NGC 6604, which triggered the star formation in M16, then M17, and further in region III possibly in the future. For the triggering mechanism we propose that a shock front due to a stellar-wind (or supernova) bubble propagates through a less dense ambient medium, not penetrating through the dense molecular cloud itself: the shock hits from outside a dense part of another cloud on the string and promotes farther condensation of gas fragments (Woodward 1975), which leads to a next star formation there. The M16 shell may be an example of such a shell directing toward the next star forming site. We suggest that M17 was excited by another shell which had expanded from M16 in the more past: the shell formation could have occurred several times at a single star forming site, as is readily indicated by the multiloop structure in the M16 shell. Such a multi-shell/bubble formation may possibly occur due to a "breathing" of the star forming activity in the course of a local sequential propagation of star formation (Elmegreen and Lada 1977) toward the dense inner part of the parent molecular cloud.

Three of us (E. F., W. R., and P. R.) gratefully thank Professor K. Akabane for kind hospitality during their stay at NRO. P.R. thanks Professor M. Morimoto for financial support by a grant from the Japanese Ministry of Education, Science, and Culture. E. F. and W. R. are grateful to the Alexander von Humboldt-Stiftung for travel grants. This work was carried out as part of an NRO-MPIfR exchange program under grants by the Japan Society for the Promotion of Science (Y. S. in 1985 and 1986).

References

Conti, P. S. 1978, *Ann. Rev. Astron. Astrophys.*, **16**, 371.
Dame, T. M. 1984, *NASA Technical Paper*, NASA TP-2288 (NASA, Scientific and Technical Information Branch, Washington, D. C.).
Downes, D., Wilson, T. L., Bieging, J., and Wink, J. 1980, *Astron. Astrophys. Suppl.*, **40**, 379.
Elliot, K. H., Goudis, C., Meaburn, J., and Pilkington, J. 1978, *Astrophys. Space Sci.*, **55**, 475.
Elmegreen, B. G. 1980, in *Giant Molecular Clouds in the Galaxy*, ed. P. M. Solomon and M. G.

Edmunds (Pergamon Press, New York), p. 19.
Elmegreen, B. G., and Lada, C. J. 1977, *Astrophys. J.*, **214**, 725.
Heiles, C. 1979, *Astrophys. J.*, **229**, 533.
Kerr, F. J. 1968, in *Nebulae and Interstellar Matter*, ed. B. M. Middlehurst and L. H. Aller (The University of Chicago Press, Chicago), p. 575.
McCray, R., and Snow, T. P., Jr. 1979, *Ann. Rev. Astron. Astrophys.*, **17**, 213.
Mezger, P. G., and Henderson, A. P. 1967, *Astrophys. J.*, **147**, 471.
Parker, R. A. R., Gull, T. R., and Kirshner, R. P. 1979, *An Emission-Line Survey of the Milky Way*, NASA SP-434 (NASA, Scientific and Technical Information Branch, Washington, D. C.), p. 17.
Reich, W. 1978, *Astron. Astrophys.*, **64**, 407.
Reich, W., Fürst, E., Steffen, P., Reif, K., and Haslam, C. G. T. 1984, *Astron. Astrophys., Suppl.*, **58**, 197.
Reynolds, R. J., and Ogden, P. M. 1979, *Astrophys. J.*, **229**, 942.
Sofue, Y., Hirabayashi, H., Akabane, K., Inoue, M., Handa, T., and Nakai, N. 1984, *Publ. Astron. Soc. Japan*, **36**, 287.
Sofue, Y., and Nakai, N. 1983, *Astron. Astrophys. Suppl.*, **53**, 57.
Sofue, Y., and Reich, W. 1979, *Astron. Astrophys. Suppl.*, **38**, 251.
Tomisaka, K., Habe, A., and Ikeuchi, S. 1981, *Astrophys. Space Sci.*, **78**, 273.
Weaver, R., McCray, R., Castor, J., Shapiro, P., and Moore, R. 1977, *Astrophys. J.*, **218**, 377.
Westerhout, G., and Wendlandt, H. U. 1982, *Astron. Astrophys. Suppl.*, **49**, 143.
Woodward, P. R. 1975, *Astrophys. J.*, **195**, 61.